Journal of Molecular Structure: THEOCHEM 960 (2010) 98–105

Contents lists available at ScienceDirect

Journal of Molecular Structure: THEOCHEM

journal homepage: www.elsevier.com/locate/theochem

Hydrogen bonding interactions in cysteine–urea complexes: Theoretical studies of structures, properties and topologies

Zhengguo Huang *, Lei Yu, Yumei Dai, Hongke Wang

Tianjin Key Laboratory of Structure and Performance for Functional Molecules, College of Chemistry, Tianjin Normal University, Tianjin 300387, People's Republic of China

ARTICLE INFO

Article history:
Received 7 June 2010
Received in revised form 24 July 2010
Accepted 24 August 2010
Available online 31 August 2010

Keywords:
Hydrogen bond
Quantum theory of atoms in molecules (QTAIM)
Natural bond orbital (NBO)
Density functional theory (DFT)
Cysteine
Urea

ABSTRACT

The hydrogen bonding interactions between cysteine and urea were studied with density functional theory (DFT) regarding their geometries, energies, vibrational frequencies, and topological features of the electron density. The quantum theory of atoms in molecules (QTAIM) and natural bond orbital (NBO) analyses were employed to elucidate the interaction characteristics in the complexes. Multiple hydrogen bonds (H-bonds) are formed in one complex since both cysteine and urea have multiple sites as H-bond donor or acceptor. Most of intermolecular H-bonds involve O atom of cysteine/urea moiety as proton acceptors. The H-bond involving O atom of urea moiety as proton acceptor and hydroxyl of cysteine moiety as proton donor is the strongest one, which is attributed to a partial covalent character. The H-bonds involving the CH group of cysteine moiety as proton donor are very weak and show small blue shifts, while other H-bonds are red-shifting ones. Both hydrogen bonding interaction and structural deformation are responsible for the stability of Cys–Urea complexes, and the complexes involving either the strongest H-bond or the smallest deformation are not the stable ones. Analysis of various physically meaningful contributions arising from the energy decomposition procedures shows that the orbital interaction of H-bond is predominant during the formation of complex. The cooperative effects happened in complexes have also been discussed. Relationships between the topological properties (electron density ρ_b and its Laplacian $\nabla^2\rho_b$) at the bond critical point (BCP) of H-bond and structural parameter (δR) as well as the second-perturbation energies $E(2)$ have also been discussed.

1. Introduction

Urea has been a widely used protein denaturant in in-vitro unfolding/refolding experiments. However, the denaturation mechanism is still not well understood. It appears that urea affects the stability of proteins both directly and indirectly. The indirect mechanism alters water structure in such a way that water becomes free to compete more successfully for backbone hydrogen bonds (H-bonds) and other intra-protein interactions. The alternative, direct mechanism may involve preferential interaction with hydrophobic residues, thereby destabilizing the hydrophobic core, or interaction with polar constituents and in particular the peptide backbone [1]. However, even within the direct mechanism there is controversy over which of the forces is dominant, electrostatic or van der Waals [2–4]. Some studies [5,6] stress the importance of urea–protein H-bonds to polar residues, while other recent studies [7,8] support an apolar urea–protein contact weakening hydrophobic effect of protein. Therefore, quantitative studies on these interactions are very useful for the interpretation of denaturation mechanism. However, such biological systems are so vast that even with the most powerful computing capabilities, no the currently quantum chemical method is within reach for the study of systems of such magnitude. An alternative approach is to quantitative study on simplified model systems at a currently viable computational level. Hence, more detailed insights into the interactions of urea with amino acids are required to understand the denaturation mechanism since amino acids are the basic structural units of protein composition. Some theoretical researches on urea–amino acid (glycine, alanine, and leucine) complexes have been reported and the results showed that there exists significantly hydrogen bonding interaction between them [4,9]. Even in such simplified model systems, the hydrogen bonding interactions are still very complicated since more than one proton donor (H-donor) and acceptor (H-acceptor) sites can be found in urea or amino acid molecule. Furthermore, it is sensible to ascribe the fundamental nature of hydrogen bonding interactions. Hence, H-bonded complexes must be considered carefully using a reliable theoretical model. MP2 method is deemed to be a reliable method for description of hydrogen bonding interactions. However, MP2 approach is not a cost-effective approach for the computation of such biomolecular

* Corresponding author.
E-mail address: hsxyhzg@126.com (Z. Huang).

0166-1280/$ - see front matter Crown Copyright © 2010 Published by Elsevier B.V. All rights reserved.
doi:10.1016/j.theochem.2010.08.029

systems even with a medium-size basis set. Although conventional density functional theory (DFT) has been accepted as a cost-effective approach for description of hydrogen bonding interactions, it cannot better describe hydrogen bonding interactions (e.g., see Refs. [10,11] and references therein) since it treat electron correlation only in an approximate manner. Recently, many methods (such as B2PLYP [12], M06L [13,14] and ωB97XD [15]) have been developed to treat hydrogen bonding and van der Waals interactions with DFT. These range from physically rigorous dispersion functionals derived from first principles to entirely empirical corrections or parametrizations. A comprehensive review of such methods is given by Johnson et al. [16]. Many studies have shown that these new DFT methods can give reliable results for a wide variety of weakly bonded systems [12,17,18].

In this work, we report the computed structural properties, electronic properties, and characteristic harmonic vibrational frequencies of H-bonds in cysteine–urea (Cys–Urea) complexes. In addition, natural bond orbital (NBO) [19,20] and the quantum theory atoms in molecules (QTAIM) [21–33] analyses were carried out so as to elucidate the hydrogen bonding interactions in Cys–Urea complexes.

2. Computational details

The ωB97XD functional from Head-Gordon and coworkers [15], includes empirical dispersion and can better treat hydrogen bonding and van der Waals interactions than conventional DFT. In this paper, the ωB97XD functional with the 6-311++G(d,p) basis set [34,35] was used. First, the geometries of the isolated cysteine and urea monomers were fully optimized. The complexes were constructed starting from the most stable cysteine and urea monomers. All complexes were also fully optimized at the same level. The counterpoise (CP) correction [36] was implemented in each step of the iterative process of geometry optimization in an integrated way in order to ensure that complexes and monomers are being computed with a consistent basis set. The harmonic vibrational frequencies were calculated with analytic second derivatives at the same level, which confirm the structures as minima and enable the evaluation of zero-point vibrational energies (ZPVE). All ZPVE and frequencies were unscaled. Finally, the interaction energies were calculated based on the ZPVE and BSSE corrections. The QTAIM and NBO analyses were also implemented to provide complementary information on the H-bond. All DFT calculations and NBO analysis were performed with the Gaussian03 [37]. The QTAIM analysis were carried out by using software AIM2000 [38] with ωB97XD wave functions employing the 6-311++G(d,p) basis set.

3. Results and discussion

Recently, conformers of cysteine [39–42] and urea [9] have been studied by different research groups. In this work, the structure of isolated cysteine and urea was well reproduced at the ωB97XD/6-311++G(d,p) level. The optimized conformers of cysteine (A) and urea (B) were presented in Fig. 1. Cysteine and urea molecules can offer several possible donor and acceptor sites to form H-bond, respectively. As shown in Fig. 1, the H-donor sites of cysteine may occur on hydroxyl (OH, O1), amino (NH_2, N), thiol group (SH, S), and even α-carbon, while carbonyl (CO, O2), amino (NH_2, N), thiol group (SH, S) as H-acceptor. Urea could offer carbonyl group (O) as H-acceptor, while amino (NH_2) as H-donor. Therefore, it seems reasonable to believe that there exist electrostatic interaction or/and hydrogen bonding interaction in amino acid–urea complex system. In contrast to merely electrostatic interactions, H-bonds are directional and lead to different configurations of complex. All optimized complexes were presented in Fig. 2, and the structural parameters of the H-bonds were listed in Table 1.

3.1. Structures

The vibrational frequency calculations show that all optimized complexes have no imaginary frequencies and are stable structures. Both inter- and intramolecular H-bonds can be characterized by the bond critical point (BCP) between H-donor (X–H) and H-acceptor (Y). The coexistences of several H-bonds maybe result in the formation of a ring structure characterized by ring critical point (RCP). Moreover, the union between BCP and corresponding RCP can be used to measure the stability of the ring structure [43]. As shown in Fig. 1 and Fig. 2, each of complexes involves multiple H-bonds. The intramolecular $O1H1^{A}\cdots N^{A}$ H-bond involved in free cysteine is characterized by corresponding BCP and RCP, and it still exist in Cys–Urea complexes except **AB4**. Compared with free cysteine, the distances between the BCP of $O1H1^{A}\cdots N^{A}$ H-bond and the corresponding RCP in these complexes have small changes, which means the intramolecular $O1H1^{A}\cdots N^{A}$ H-bond is stable and no bond cleavage happened. The intramolecular $SH2^{A}\cdots O2^{A}$ H-bond can be found in **AB4**, while **AB2** involves the intramolecular $NH3^{A}\cdots S^{A}$ H-bond. However, the $NH3^{A}\cdots S^{A}$ and $SH2^{A}\cdots O2^{A}$ H–bonds cannot compare with the $O1H1^{A}\cdots N^{A}$ H-bond in strength because of the shorter distances between the BCPs and corresponding RCPs. Therefore, two intramolecular H-bonds are involved in **AB2**, while other complexes have one intramolecular H-bond, respectively. In addition, the $SH2^{A}\cdots O2^{A}$ H-bond take the place of

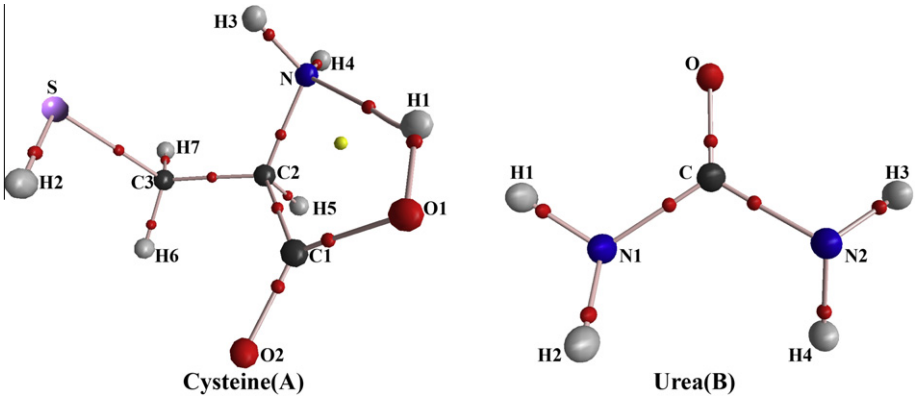

Fig. 1. Molecular graphs of free cysteine and urea monomers. Large circles correspond to attractors attributed to atomic positions: gray, H; blue, N; black, C; red, O; purple, S. Small circles are attributed to critical points: red, bond critical point; yellow, ring critical point. (For interpretation of the references to color in this figure legend, the reader is referred to the web version of this article.)

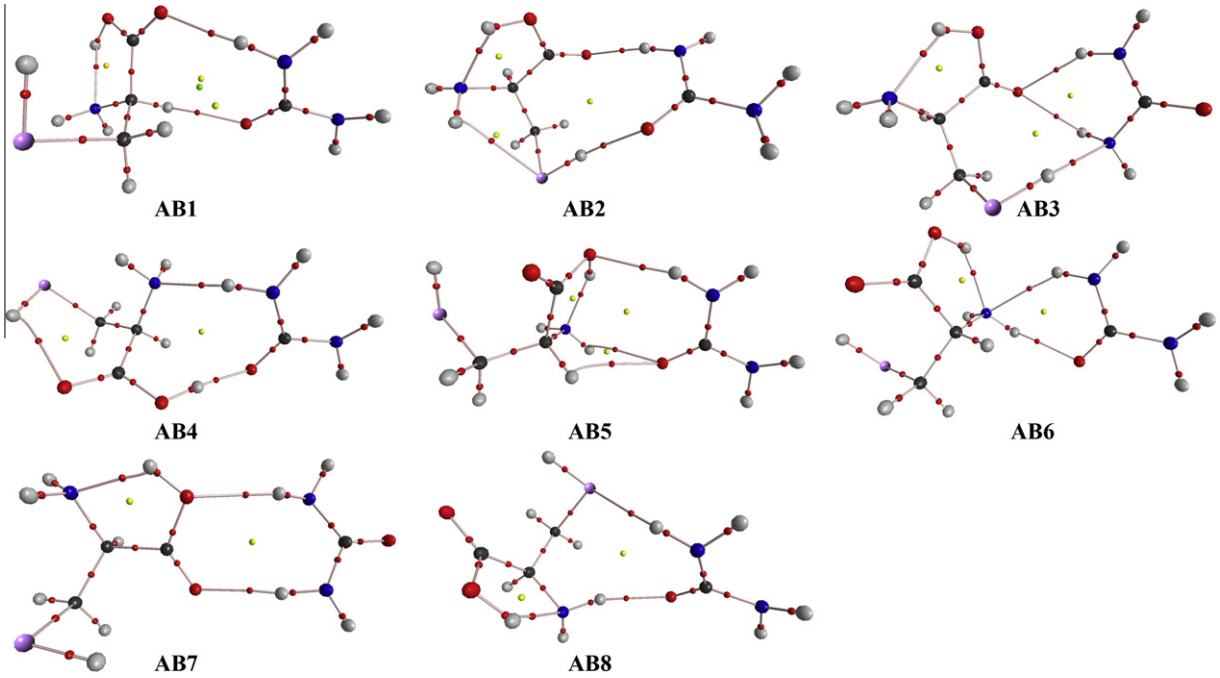

Fig. 2. Molecular graphs of Cys–Urea complexes. Large circles correspond to attractors attributed to atomic positions: gray, H; blue, N; black, C; red, O; yellow, S. Small circles are attributed to critical points: red, bond critical point; yellow, ring critical point; green, cage critical point. The left part is unit A (cysteine) and the right part is unit B (urea). (For interpretation of the references to color in this figure legend, the reader is referred to the web version of this article.)

Table 1
Structural parameters (bond lengths in Å, angles in degree) of H-bonds in Cys–Urea complexes at ωB97XD/6-311++G(d, p) level.

Complex	H-Bond[a]	R_{X-H}	$R_{H\cdots Y}$	ΔR_{X-H}[b]	δR	∠X–H···Y
AB1	$N1H1^{B}\cdots O2^{A}$	1.018	1.925	0.011	0.795	175.7
	$C2H5^{A}\cdots O^{B}$	1.096	2.212	−0.001	0.508	138.0
	$O1H1^{A}\cdots N^{A}$	0.983	1.869	0.005	0.881	126.3
AB2	$SH2^{A}\cdots O^{B}$	1.356	1.976	0.011	0.744	168.9
	$N1H1^{B}\cdots O2^{A}$	1.016	1.927	0.009	0.793	168.2
	$O1H1^{A}\cdots N^{A}$	0.983	1.871	0.005	0.879	126.3
	$NH3^{A}\cdots S^{A}$	1.018	2.574	0.001	0.426	116.7
AB3	$N2H4^{B}\cdots O2^{A}$	1.009	2.157	0.002	0.563	146.9
	$N1H2^{B}\cdots O2^{A}$	1.011	2.245	0.004	0.475	129.8
	$SH2^{A}\cdots N1^{B}$	1.355	2.207	0.010	0.543	165.3
	$O1H1^{A}\cdots N^{A}$	0.983	1.868	0.005	0.882	125.7
AB4	$O1H1^{A}\cdots O^{B}$	0.989	1.675	0.011	1.045	174.2
	$N1H1^{B}\cdots N^{A}$	1.025	1.976	0.018	0.774	162.6
	$SH2\cdots O2^{A}$	1.344	2.308	-0.001	0.412	121.6
AB5	$N1H1^{B}\cdots O1^{A}$	1.011	2.103	0.004	0.617	161.0
	$NH4^{A}\cdots O^{B}$	1.011	2.359	0.000	0.361	117.1
	$C2H5^{A}\cdots O^{B}$	1.094	2.474	−0.003	0.246	114.4
	$O1H1^{A}\cdots N^{A}$	0.992	1.791	0.014	0.959	130.0
AB6	$N1H1^{B}\cdots N^{A}$	1.010	2.355	0.003	0.395	138.2
	$NH4^{A}\cdots O^{B}$	1.019	2.048	0.008	0.672	144.6
	$O1H1^{A}\cdots N^{A}$	0.977	1.910	-0.001	0.84	125.8
AB7	$N2H4^{B}\cdots O2^{A}$	1.012	2.060	0.005	0.660	172.4
	$N1H2^{B}\cdots O1^{A}$	1.009	2.200	0.002	0.520	164.1
	$O1H1^{A}\cdots N^{A}$	0.983	1.885	0.005	0.865	125.0
AB8	$NH3^{A}\cdots O^{B}$	1.022	1.955	0.005	0.765	163.0
	$N1H1^{B}\cdots S^{A}$	1.013	2.561	0.006	0.439	158.0
	$O1H1^{A}\cdots N^{A}$	0.986	1.841	0.008	0.909	128.2
Cys	$O1H1^{A}\cdots N^{A}$	0.978	1.917		0.833	124.6
	SH2	1.345				
	NH4	1.011				
	NH3	1.017				
	C2H5	1.097				
Urea	N1H1	1.007				
	N1H2	1.007				

[a] Superscript "A" denote cysteine and "B" denote urea.
[b] $\Delta R_{X-H} = R_{X-H}$ (complexes) − R_{X-H}(free monomer).

$O1H1^{A}\cdots N^{A}$ H-bond in **AB4**, which indicate that serious deformation happened and made against the stability of the complexes. In conclusion, $O1H1^{A}\cdots N^{A}$ H-bond is the dominating intramolecular H-bonds in Cys–Urea complexes.

Besides above intramolecular H-bonds, different intermolecular H-bonds in Cys–Urea complexes can be characterized by BCPs and corresponding RCPs as well. Each of complexes involves two or three intermolecular H-bonds. As shown in Fig. 2, major intermolecular H-bonds in complexes involve hydroxyl (cysteine) and amino (cysteine or urea) as H-donor. Few intermolecular H-bonds involve thiol group (SH, S) as well α-carbon (C2H5) in cysteine as H-donor. Such H-bonds include $SH2^{A}\cdots O^{B}$, $SH2^{A}\cdots N1^{B}$ and $C2H5^{A}\cdots O^{B}$, which are regarded as weak H-bonds. In addition, a bifurcate H-bond consisted of $N1H2^{B}\cdots O2^{A}$ and $N2H4^{B}\cdots O2^{A}$ H-bonds can be found in **AB3**, while another bifurcate H-bond formed by $NH4^{A}\cdots O^{B}$ and $C2H5^{A}\cdots O^{B}$ H-bonds are involved in **AB5**. The bifurcate H-bond in **AB6** are formed by intermolecular $N1H1^{B}\cdots N^{A}$ and interamolecular $O1H1^{A}\cdots N^{A}$ H-bond.

Structural parameters of H-bonds can give preliminary information on the nature of H-bonds. From the viewpoint of the structural parameter of H-bond, electrons transfer happen between X–H and Y group during the process of the formation of X–H···Y H-bond, which results in the shortening of H···Y bond length and the elongation of X-H bond length. As shown in Table 1, the intermolecular H-bond including $N1H1^{B}\cdots N^{A}$ in **AB4** should be the strongest H-bond since the change of bond length (0.018 Å of $\Delta R_{N1-H1^{B}}$) is the largest among H-bonds, while another H-bond ($O1H1^{A}\cdots O^{B}$) of **AB4** is also stronger since it involves a second largest ΔR_{X-H} (0.011 Å). Therefore, **AB4** seems to be the most stable complex due to the two strong H-bond, however, the stability of is weaken by the bond cleavage of the intramolecular $O1H1^{A}\cdots N^{A}$ H-bond, which will be further discussed later. In addition, the $C2H5^{A}\cdots O^{B}$ H-bond in **AB1** as well as **AB5** involves a negative ΔR_{X-H} value of −0.001and −0.001, respectively, which should be a blue-shifting H-bond. Besides X–H bond length of H-bond, the H···Y bond length

represent the strength o H-bond as well. However, because of different atom as H-acceptor in different H-bonds, the H···Y bond length cannot be used directly, so a H-bond parameter, δR [44], is defined as

$$\delta R_{H\cdots Y} = R_H^{vDW} + R_Y^{vDW} - R_{H\cdots Y} \quad (1)$$

where R_H^{vDW} and R_Y^{vDW} are van der Waals radii of H and Y atoms given by Bondi [45], respectively, $R_{H\cdots Y}$ is the length of the H-bond (H···Y). As shown in Table 1, the maximum of $\delta R_{H\cdots Y}$ is 1.045 Å for the intermolecular O1H1$^{A}\cdots$O^{B} H-bond in **AB4**, in which the $\delta R_{H\cdots Y}$ (0.774 Å) of another intermolecular H-bond (N1H1$^{B}\cdots$N^{A}) is larger than those of most H-bonds in other complexes as well. Therefore, it can be learned that the strongest hydrogen bonding interaction happened in **AB4**, which is consistent with above discussion. The smallest $\delta R_{H\cdots Y}$ value of 0.246 Å is involved in the C2H5$^{A}\cdots$O^{B} H-bond in **AB5**, which should be a weak H-bond.

As shown in Table 1, for the intramolecular O1H1$^{A}\cdots$N^{A} H-bond in all complexes except **AB4**, the R_{N1-H1} bond length is elongated and $\delta R_{H\cdots Y}$ is larger than that of free cysteine, which indicate that the strength of intramolecular O1H1$^{A}\cdots$N^{A} H-bond is enhanced. Especially, the strongest intramolecular O1H1$^{A}\cdots$N^{A} H-bond is found in **AB5** which can be learned from the largest ΔR_{N1-H1} and $\delta R_{H\cdots Y}$ values. The enhancement of the O1H1$^{A}\cdots$N^{A} H-bond is attributed to the cooperative effect which exists among multiple H-bond in complexes. Cooperativity, that is, the enhancement of the first hydrogen bond (HB) between a proton donor and a proton acceptor when a second HB is formed between one of these two species and a third partner, is one of the hallmarks of hydrogen bonding [46–48]. As shown in Fig. 2, for some complexes (**AB2**, **AB5**, **AB6** and **AB8**), the N atom of cysteine becomes a stronger acceptor if the amino donate an H-bond, the same effects also occur in **AB5** and **AB7** in which the hydroxyl O atom of cysteine moiety becomes a stronger donor when it accept an H-bond. Moreover, the stronger donor and the stronger acceptor lead to the strongest intramolecular O1H1$^{A}\cdots$N^{A} H-bond in **AB5**. In addition, the cooperative effect also occurs in **AB3** where the amino of urea moiety form H-bonds with carbonyl O atom as well as thiol group of cysteine moiety simultaneously.

3.2. Vibrational frequencies

The frequency of H-bonds in Cys–Urea complex and monomers as well as their shifts were listed in Table 2. The red-shifts in the X–H stretching frequency have been traditionally considered one of the main fingerprints of H-bonds, assuming that formation of an H-bond weakens an X–H single bond. However, it is not easily to calculate the shifts of X–H stretching vibrational modes if it mixes with other vibrational modes. As shown in Table 2, the strong mixture among the asymmetric and symmetric H–N–H stretching vibrational modes can be found in free urea molecules. Due to the strong mixture, four shift values are given for each amino stretching vibration modes of urea moiety in complex. Similar things also happened in Cys–Urea complexes. For example, the frequencies of 3364.1 and 3323.2 cm^{-1} in **AB4** are assigned to the combined O1–H1 stretching vibration of cysteine moiety with the symmetric H–N–H stretching vibration of one amino group in urea moiety. As a result, two $\Delta\upsilon_{X-H}$ values were given with respect to the O1–H1 stretching vibrational mode of free cysteine, while four $\Delta\upsilon_{X-H}$ values were given with respect to the four vibrational modes derived from the coupling of the asymmetric and symmetric H–N–H stretching vibrational modes of free urea molecule. Moreover, for the O1H1$^{A}\cdots$O^{B} and N1H1$^{B}\cdots$N^{A} H-bonds in **AB4**, the red shifted of about −200 to −300 cm^{-1} are larger than those of other H-bonds, so the two H-bonds are the two strongest red-shifting ones, which is consistent with above discussion. The red shifts of H-bonds in other complexes vary from tens to about one hundred wavenumbers, so generally believe that they are weaker than those of **AB4**. In addition, the C2H5$^{A}\cdots$O^{B} H-bond in **AB1** and **AB5** should be blue-shifting H-bond with positive shift of 18.8 and 24.7 cm^{-1}, respectively.

3.3. QTAIM analysis

To quantitatively study the nature of H-bond, QTAIM analysis has been carried out since the structural parameters can only give us some preliminary qualitative information of H-bond. QTAIM has been proved to be a very useful tool in describing electron densities in H-bond systems [44,49–53]. Especially, according to QTAIM theory, Koch and Popelier proposed a set of criteria for the existence of H-bond [54]. The criteria provide a basis to distinguish these inter-

Table 2
The X–H stretching frequencies (cm^{-1}) of Cys–Urea complexes and free monomers calculated at ωB97XD/6-311++G(d,p) level.

Complex	H-Bond	υ_{X-H}[a,b]	$\Delta\upsilon_{X-H}$[b]
AB1	N1H1$^{B}\cdots$O2^{A}	3704.8(89, a), 3497.4(353, s)	−34.1(sa), −33.4(aa), −126.9(ss), −122.2(as)
	C2H5$^{A}\cdots$O^{B}	3082.2(29)	18.8
AB2	SH2$^{A}\cdots$O^{B}	2598.2(344)	−124.3
	N1H1$^{B}\cdots$O2^{A}	3720.7(100, a), 3519.9(315, s)	−18.2(sa), −17.5(aa), −104.4(ss), −99.7(as)
AB3	N2H4$^{B}\cdots$O2^{A}	3760.1(109, a), 3606.9(118, s)	21.2(sa), 21.9(aa), −17.4(ss), −12.7(as)
	N1H2$^{B}\cdots$O2^{A}	3712.5(60, a), 3589.3(19, s)	−26.4(sa), −25.7(aa), −35(ss), −30.3(as)
	SH2$^{A}\cdots$N1^{B}	2623.5(245)	−99
AB4	O1H1$^{A}\cdots$O^{B}	3364.1(2047), 3323.2(208)[c]	−208.7, −249.6[d]
	N1H1$^{B}\cdots$N^{A}	3364.1(2047), 3323.2(208)[c]	−260.2(ss), −255.5(as), −301.1(ss), −296.4(as)
AB5	N1H1$^{B}\cdots$O1^{A}	3735.7(111, a), 3587.1(209, s)	−3.2(sa), −2.5(aa), −37.2(ss), −32.5(as)
	NH4$^{A}\cdots$O^{B}	3667.3(64, a), 3563.8(2, s)	−77.5(a), 34(s)
	C2H5$^{A}\cdots$O^{B}	3088.1(3)	24.7
AB6	N1H1$^{B}\cdots$N^{A}	3729.3(100, a), 3596.8(89, s)	−9.6(sa), −8.9(aa), −27.5(ss), −22.8(as)
	NH4$^{A}\cdots$O^{B}	3564.0(103, a), 3474.9(124, s)	−166.4(a), −54.9(s)
AB7	N2H4$^{B}\cdots$O2^{A}	3735.8(117, a), 3606.1(103, s)	−3.1(sa), −2.4(aa), −18.2(ss), −13.5(as)
	N1H2$^{B}\cdots$O1^{A}	3730.3(103, a), 3570.7(186, s)	−8.6(sa), −7.9(aa), −53.6(ss), −48.9(as)
AB8	NH3$^{A}\cdots$O^{B}	3456.3(132), 3425.0(542.8)[c]	−216.3(a), −104.8(s)
	N1H1$^{B}\cdots$S^{A}	3710.6(1012, a), 3555.3(274, s)	−28.3(sa), −27.6(aa), −69(ss), −64.3(as)
Cys	NH_2	3641.3(20, a), 3529.8(27, s)	
	S–H2	2722.5(0)	
	O1–H1	3572.8(252)	
	C2–H5	3063.4(9)	
Urea	N–H	3738.9(48, sa), 3738.2(31, aa), 3624.3(5, ss), 3619.6(57, as)	

[a] Numbers in parentheses are intensity (km mol^{-1}) of vibrational modes.
[b] "s" denote symmetric stretching vibrational modes, and "a" denote asymmetric stretching vibrational modes. Numbers in parentheses are intensity (in km mol^{-1}) of vibrational modes. For the vibrational modes of free urea molecule, the vibrational modes of two NH_2 groups mix with each other, so the first "s" (or "a") represents the total symmetry of urea molecule, while the second "s" (or "a") represents the symmetry of each of NH_2 group.
[c] The strong mixture exist between the O1–H1 stretching of cysteine moiety and the symmetric H1N1H2 stretching of urea moiety.
[d] The first two $\Delta\upsilon_{X-H}$ correspond to the O1–H1 stretching virbrational model of free cysteine, and the last two $\Delta\upsilon_{X-H}$ correspond to the symmetric H1N1H2 stretching mode of free urea.

actions from van der Waals interactions and have been proved to be valid for standard and nonconventional H-bonds. The results of QTAM analysis were listed in Table 3.

According to QTAIM, electron density (ρ_b) at the BCP of XH···Y H-bond is used to describe the strength of H-bond. In the light of the criteria established by Popelier, ρ_b must fall between 0.002 and 0.04 a.u. for a H-bond to be formed [22]. The ρ_b (0.04617) of the O1H1^{A}··O^{B} H-bond in **AB4** is beyond the upper-limit of the range which indicate that a partial covalent character is attributed to the H-bonds. Therefore, the O1H1^{A}··O^{B} H-bond in **AB4** is the strongest due to the largest ρ_b, which is consistent with above discussion from the viewpoint of structure. All ρ_b values of other H-bonds are within the range, while the smallest ρ_b of the C2H5^{A}···O^{B} H-bond in **AB5** indicate that it is one of the weakest H-bond. Generally, the ρ_b decreases as a result of the elongation of the corresponding bond. The opposite occurs when the bond length shorten. Therefore, a relationship between ρ_b and H···Y bond length of X–H···Y H-bond is predictable. Because of different atoms as H-acceptor in different H-bonds, the H-bond parameter $\delta R_{H\cdots Y}$ defined in Eq. (1) is used to replace H···Y bond length to carry out correlation analysis. As shown in Fig. 3, a good linear relationship between $\ln\rho_b$ and $\delta R_{H\cdots Y}$ was found and the fitted equation can be expressed as

$$\ln \rho_b = -5.1236 + 1.8688\delta R_{H\cdots Y} r = 0.9705 \quad (2)$$

The BCP local energy densities may be used to characterize the hydrogen bonding interaction [21,22]. Based on the virial theorem in the BCP, the total energy density, H_b, can be expressed as

$$(1/4)\nabla^2\rho_b = 2G_b + V_b \quad (3)$$

$$H_b = G_b + V_b \quad (4)$$

where G_b (always positive) and V_b (always negative) are the kinetic and potential energy densities, respectively. The sign of H_b will depend on which contribution, potential or kinetic, will locally prevail on the BCP. $H_b < 0$ reflects a prevalence of the potential energy,

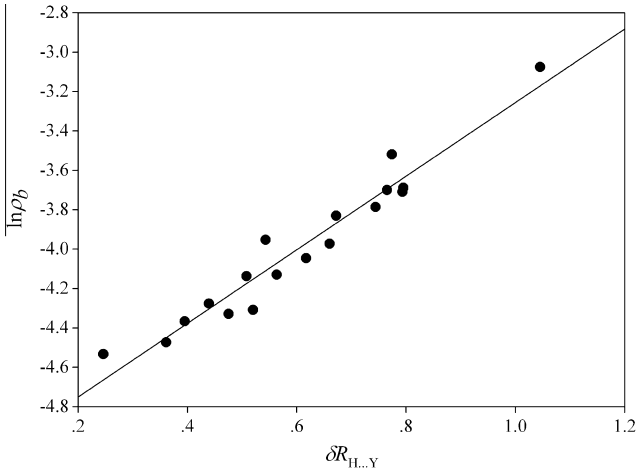

Fig. 3. Correlation between the electron density at the BCPs in the logarithmic value ($\ln\rho_b$) and the H-bond parameter δR.

which is a consequence of the stabilization of the accumulated electron charge, a typical feature of covalent interactions [55,56]. In this way, a partial covalent character is attributed to the H-bonds exhibiting $H_b < 0$. Moreover, the Laplacian of the electron density at the BCP ($\nabla^2\rho_b$) is low and positive, which is typical of closed-shell interactions. Therefore, the following criterion of strength was proposed by Popelier [54]: for weak H-bonds, $\nabla^2\rho_b > 0$ and $H_b > 0$; for H-bonds of medium strength, $\nabla^2\rho_b > 0$ and $H_b < 0$; for strong H-bonds, $\nabla^2\rho_b < 0$ and $H_b < 0$. This classification shows that weak H-bonds eventually merge with (weaker) van der Waals interactions whereas strong H-bonds merge, at the other end of the continuum, with covalent and polar bonds.

According to the criteria of H-bonds proposed by Popelier, all H-bonds of the studied complexes have positive $\nabla^2\rho_b$ values and fall within the 0.02–0.15 a.u. range [43,54]. As shown in Table 3, the O2H1^{A}···O^{B} H-bond in **AB4** involve the largest value of $\nabla^2\rho_b$

Table 3
Topological Properties (in a.u.) of the BCPs of intermolecular H-bonds in Cys–Urea complexes obtained from the ωB97XD/6-311++G(d, p) level calculations.

Complex	H-bond	ρ_b	$\nabla^2\rho_b$	V_b	G_b	H_b
AB1	N1H1^{B}···O2^{A}	0.02502	0.09405	−0.01865	0.02108	0.00243
	C2H5^{A}···O^{B}	0.01598	0.05602	−0.01010	0.01205	0.00195
	O1H1^{A}···N^{A}	0.03948	0.11250	-0.03418	0.03115	-0.00303
AB2	SH2^{A}···O^{B}	0.02269	0.08474	−0.01512	0.01815	0.00303
	N1H1^{B}···O2^{A}	0.02451	0.09371	−0.01828	0.02085	0.00257
	O1H1^{A}···N^{A}	0.03925	0.11200	-0.03388	0.03094	-0.00294
	NH3^{A}···S^{A}	0.01571	0.04962	-0.00962	0.01101	0.00139
AB3	N2H4^{B}···O2^{A}	0.01609	0.05742	−0.01047	0.01241	0.00194
	N1H2^{B}···O2^{A}	0.01318	0.05114	−0.00889	0.01084	0.00195
	SH2^{A}···N1^{B}	0.01921	0.05126	−0.00985	0.01133	0.00148
	O1H1^{A}···N^{A}	0.03951	0.11265	-0.03425	0.03120	-0.00304
AB4	O1H1^{A}···O^{B}	0.04617	0.14176	−0.04404	0.03974	−0.0043
	N1H1^{B}···N^{A}	0.02964	0.08291	−0.02057	0.02065	0.00008
	SH2^{A}···O2^{A}	0.01490	0.04864	-0.00956	0.01086	0.0013
AB5	N1H1^{B}···O1^{A}	0.01750	0.06273	−0.01492	0.01359	−0.00133
	NH4^{A}···O^{B}	0.01142	0.04502	−0.00789	0.00957	0.00168
	C2H5^{A}···O^{B}	0.01075	0.03759	−0.00696	0.00818	0.00122
	O1H1^{A}···N^{A}	0.04707	0.11668	-0.04292	0.03604	-0.00688
AB6	N1H1^{B}···N^{A}	0.01270	0.04185	−0.00709	0.00877	0.00168
	NH4^{A}···O^{B}	0.02171	0.07667	−0.01512	0.01714	0.00202
	O1H1^{A}···N^{A}	0.03592	0.10814	-0.03026	0.02865	-0.00161
AB7	N2H4^{B}···O2^{A}	0.01883	0.07033	−0.01263	0.01510	0.00247
	N1H2^{B}···O1^{A}	0.01346	0.05083	−0.00852	0.01061	0.00209
	O1H1^{A}···N^{A}	0.03814	0.11090	-0.03257	0.03015	-0.00242
AB8	NH3^{A}···O^{B}	0.02473	0.09025	−0.01809	0.02033	0.00224
	N1H1^{B}···S^{A}	0.01390	0.03751	−0.00659	0.00798	0.00139
	O1H1^{A}···N^{A}	0.04232	0.11370	-0.03724	0.03283	-0.00441
Cysteine	O1H1^{A}···N^{A}	0.03553	0.10845	-0.02983	0.02847	-0.00136

(0.14176) as well as the minimum of H_b (−0.00133), which indicates that it is the strongest H-bond among Cys–Urea complexes and a partial covalent character is attributed to the H-bonds. Similarly, according to above criterion, all other H-bonds should belong to the H-bond of medium strength. Moreover, a regression analysis has been carried out to investigate the relationship between $\nabla^2\rho_b$ and structural parameters. The fitted curve was shown in Fig. 4 and the fitted equation can be expressed as

$$\ln\nabla^2\rho_b = -3.8652 + 1.8452\delta R_{\mathrm{H}\cdots\mathrm{Y}}\, r = 0.9750 \quad (5)$$

It is easily to found that good linear relationships exist between ln $\nabla^2\rho_b$ and $\delta R_{\mathrm{H}\cdots\mathrm{Y}}$.

The cooperativity of H-bond in complexes can be learned from the results of QTAIM as well. As shown in Table 3, the values of ρ_b as well as $\nabla^2\rho_b$ of the intramolecular O1H1$^{\mathrm{A}}\cdots$N$^{\mathrm{A}}$ H-bond in complexes are larger than those of free cysteine, which is attributed to the cooperative effect. Moreover, the values of (0.04707) and $\nabla^2\rho_b$ (0.11668) of the intramolecular O1H1$^{\mathrm{A}}\cdots$N$^{\mathrm{A}}$ H-bond in **AB5** are the largest ones among complexes, which indicates the strong cooperative effect occurs in **AB5** and is consistent with above discussion. In addition, since the values of ρ_b of the intramolecular O1H1$^{\mathrm{A}}\cdots$N$^{\mathrm{A}}$ H-bond in **AB5** and **AB8** are beyond the upper-limit of the range the H-bonds attribute to a partial covalent character, which is further confirmed by the negative H_b values of **AB5** and **AB8**.

3.4. NBO analysis and energy

The formation of H-bond implies that a certain amount of electronic charge is transferred from the H-acceptor to the H-donor, and a rearrangement of electron density within each part of molecule is occurred. Although QTAIM analysis can provide relevant information on the strength of H-bonds in Cys–Urea complexes, it cannot give us information on electronic charge transfer, which can be given by NBO analysis. Therefore, the NBO analysis was also performed here to deepen the nature of H-bonds and the result was listed in Table 4. According to NBO theory [19], charge transfer or electron delocalization effects can be treated by the second-perturbation energies $E(2)$

$$E(2) = -n_\sigma \frac{\langle\sigma|F|\sigma^*\rangle}{\varepsilon_{\sigma^*} - \varepsilon_\sigma} = -n_\sigma \frac{F_{ij}^2}{\Delta\varepsilon} \quad (6)$$

where F_{ij} is the Fock matrix element between the NBO i (σ) and j (σ^*), ε_σ and ε_{σ^*} are the energies of σ and σ^* NBOs, and n_σ is the population. Therefore, $E(2)$ lowering is responsible for the orbital interaction of H-bond.

Table 4
The second-perturbation energies $E(2)$ (in kcal mol^{-1}) of intermolecular H-Bonds in Cys–Urea complexes.

Complex	H-bond	$E(2)$[a]	Complex	H-bond	$E(2)$[a]
AB1	N1H1$^{\mathrm{B}}\cdots$O2$^{\mathrm{A}}$	4.73(5.99)	**AB5**	N1H1$^{\mathrm{B}}\cdots$O1$^{\mathrm{A}}$	1.40(4.26)
	C2H5$^{\mathrm{A}}\cdots$O$^{\mathrm{B}}$	1.79(1.47)		NH4$^{\mathrm{A}}\cdots$O$^{\mathrm{B}}$	0.41
	O1H1$^{\mathrm{A}}\cdots$N$^{\mathrm{A}}$	16.80		C2H5$^{\mathrm{A}}\cdots$O$^{\mathrm{B}}$	0.22
AB2	SH2$^{\mathrm{A}}\cdots$O$^{\mathrm{B}}$	6.35(3.88)		O1H1$^{\mathrm{A}}\cdots$N$^{\mathrm{A}}$	24.35
	N1H1$^{\mathrm{B}}\cdots$O2$^{\mathrm{A}}$	4.45(4.52)	**AB6**	N1H1$^{\mathrm{B}}\cdots$N$^{\mathrm{A}}$	2.45
	O1H1$^{\mathrm{A}}\cdots$N$^{\mathrm{A}}$	16.63		NH4$^{\mathrm{A}}\cdots$O$^{\mathrm{B}}$	1.82(5.15)
	NH3$^{\mathrm{A}}\cdots$S$^{\mathrm{A}}$	3.00		O1H1$^{\mathrm{A}}\cdots$N$^{\mathrm{A}}$	13.52
AB3	N2H4$^{\mathrm{B}}\cdots$O2$^{\mathrm{A}}$	0.92(2.52)	**AB7**	N2H4$^{\mathrm{B}}\cdots$O2$^{\mathrm{A}}$	2.80(4.25)
	N1H2$^{\mathrm{B}}\cdots$O2$^{\mathrm{A}}$	0.95(0.10)		N1H2$^{\mathrm{B}}\cdots$O1$^{\mathrm{A}}$	2.56(0.38)
	SH2$^{\mathrm{A}}\cdots$N1$^{\mathrm{B}}$	9.32		O1H1$^{\mathrm{A}}\cdots$N$^{\mathrm{A}}$	15.60
	O1H1$^{\mathrm{A}}\cdots$N$^{\mathrm{A}}$	16.65	**AB8**	NH3$^{\mathrm{A}}\cdots$O$^{\mathrm{B}}$	3.65(6.43)
AB4	O1H1$^{\mathrm{A}}\cdots$O$^{\mathrm{B}}$	8.64(19.47)		N1H1$^{\mathrm{B}}\cdots$S$^{\mathrm{A}}$	1.33(5.78)
	N1H1$^{\mathrm{B}}\cdots$N1$^{\mathrm{A}}$	17.92		O1H1$^{\mathrm{A}}\cdots$N$^{\mathrm{A}}$	19.75
	SH2$^{\mathrm{A}}\cdots$O2$^{\mathrm{A}}$	0.59(1.89)	Cysteine	O1H1$^{\mathrm{A}}\cdots$N$^{\mathrm{A}}$	13.17

[a] The values are O (or S) sp hybrid branch to form the H-bond; those in the parentheses are O (or S) p hybrid branch. The lone pair of N atom is mainly of p character. See discussion in the text.

As shown in Table 4, the O (and S) atom involved in H-bond has two branches: one has sp hybrid characteristics, and the other one has more p hybrid characteristics; they corresponds to two $E(2)$ values, respectively. In contrast to the O (S) atoms, the N atom shows p characteristics in H-bonds. Thereby, the O (S) atoms exhibit more flexibility (less anisotropic) than the N atom in H-bond. The two largest $E(2)$ value of 28.11 and 17.92 kcal mol^{-1} are found for the O1H1$^{\mathrm{A}}\cdots$O$^{\mathrm{B}}$ and N1H1$^{\mathrm{B}}\cdots$N$^{\mathrm{A}}$ H-bonds in **AB4**, respectively, which indicates the strongest charge-transfer effect happened in **AB4**. In addition, the relationship between $E(2)$ and ρ_b was also investigated since $E(2)$ is responsible for orbital interaction of H-bond, the results show that the $E(2)$ linearly depend on ρ_b as shown in Fig. 5 and the relationship can be expressed as

$$E(2) = 7.8852 + 777.2065\rho_b \quad r = 0.9697 \quad (7)$$

In addition, the results of NBO can also give evidence for the cooperativity of H-bond in complexes. As shown in Table 4, the values of $E(2)$ of the intramolecular O1H1$^{\mathrm{A}}\cdots$N$^{\mathrm{A}}$ H-bond in complexes are larger than those of free cysteine, which is attributed to the cooperative effect. Moreover, the strong cooperative effect occurs

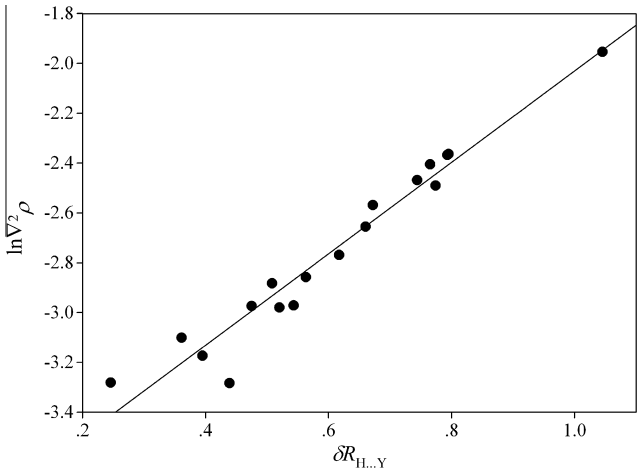

Fig. 4. Correlation between the logarithmic Laplacian of the electron density ($\ln\nabla^2\rho_b$) at the BCPs of H-bonds and the H-bond parameter δR.

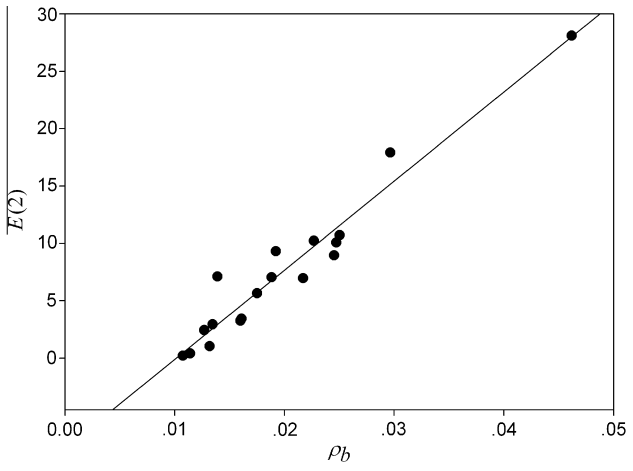

Fig. 5. Correlation between the second-perturbation energies $E(2)$ (the sum of sp and p branch for O atom, in kcal mol^{-1}) and the electron density (ρ_b) at BCPs of H-bonds.

in **AB5** is confirmed by the largest $E(2)$ value of 24.35 kcal mol^{-1} of the intramolecular O1H1$^{A}\cdots$N^{A} H-bond, which also agree with above discussion.

To estimate the total charge-transfer (CT) effects between cysteine and urea moiety in complexes, the CT energy (ΔE_{CT}) can be obtained by summarizing $E(2)$ for intermolecular H-bonds, as proposed by Reed et al. [20]. In the NBO scheme, ΔE_{CT} account for the orbital interaction and polarization interactions of H-bond, while ΔE_{NCT} of H-bond consists of the classical electrostatic interaction and the Pauli steric repulsion interaction, and the sum of ΔE_{CT} and ΔE_{NCT} is the actual interaction energy (ΔE_{int}) [19].

$$\Delta E_{int} = \Delta E_{NCT} + \Delta E_{CT} \quad (8)$$

Therefore, ΔE_{int} represents the influence of H-bond on the binding energy (ΔE) of Cys–Urea complexes. On the basis of NBO theory, ΔE is also influenced by the deformation of the cysteine and urea monomers except for ΔE_{int}, so ΔE can be decomposed as

$$\Delta E = \Delta E_{prep} + \Delta E_{int} \quad (9)$$

where the ΔE_{prep} is the preparation energy. Namely,

$$\Delta E_{prep} = E_{Cys\cdots Urea} - E_{Cys(Urea)} - E_{Urea(Cys)} \quad (10)$$

$$\Delta E_{int} = E_{Cys\cdots Urea} - E_{Cys} - E_{Urea} \quad (11)$$

where $E_{Cys\cdots Urea}$ is the energy of Cys–Urea complex, $E_{Cys(Urea)}$ is the energy of cysteine monomer when all the nucleus structure units of urea are considered as puppet atoms of carrying empty orbital; $E_{Urea(Cys)}$ is the energy of urea monomer when all the nucleus structure units of cysteine are considered as puppet atoms of carrying empty orbital; E_{Cys} is the energy of the most stable cysteine molecule; E_{Urea} is the energy of the most stable urea molecule. Generally speaking, the value of ΔE_{prep} should be a positive value because the structural deformation brings the molecular energy to a higher energy level, and the ΔE_{int} should be a negative value unless the complex is less stable than the monomers.

On the basis of the NBO analyses, the binding energies ΔE of Cys–Urea complexes were decomposed into several terms summarized in Table 5. Since the intramolecular O1H1$^{A}\cdots$N^{A} H-bond still exist in all Cys–Urea complexes except **AB4**, these complexes are predicted to have small deformation, while the O1H1$^{A}\cdots$N^{A} H-bond in **AB4** is destroyed and lead to serious deformation which is responsible for the largest ΔE_{prep} value (10.77 kcal mol^{-1}). The serious deformation in **AB4** counteracts the strongest hydrogen bonding interaction (ΔE_{int} = −46.03 kcal mol^{-1}) to a great extent. Therefore, **AB4** is not the most stable complex. In fact, the positive binding energy ΔE (2.42 kcal mol^{-1}) of **AB4** makes against the stability. On the other hand, the smallest ΔE_{prep} (0.32 kcal mol^{-1}) also do not means that **AB7** is the most stable complex since both intermolecular H-bonds of **AB7** are weaker. **AB1** is the most stable complex which involve one strong N1H1$^{B}\cdots$O2^{A} H-bond as well as one weak C2H5$^{A}\cdots$O^{B} H-bonds, more importantly, its deformation is small. Therefore, both hydrogen bonding interaction and structural deformation are important factors for the stability of Cys–Urea complexes. In addition, as shown in Table 5, for all Cys–Urea complexes, ΔE_{CT} is larger than ΔE_{NCT}, because the hydrogen bonding interaction is a short-distance force, while the electrostatic interaction is a long-distance force; namely, the former should be predominant as two monomers get together. Unlike other complex, the negative value of ΔE_{NCT} (−1.99 kcal ol^{-1}) of **AB5** make positive contribution to ΔE_{int} and in favor of the stability of **AB5**.

Table 5
Total energy (E), Preparation Energies (ΔE_{prep}), Charge-Transfer Energies (ΔE_{CT}), Non-Charge-Transfer Energies (ΔE_{NCT}), Interaction Energies (ΔE_{int}), and Binding Energies (ΔE) of Cys–Urea complexes calculated at ωB97XD/6-311++G(d,p) level.

Complex	E[a]	ΔE_{int}	ΔE_{prep}	ΔE_{CT}	ΔE_{NCT}	ΔE
AB1	−947.063966	−10.05	0.79	−13.98	3.93	−9.26
AB2	−947.061959	−8.79	1.09	−19.20	10.41	−7.70
AB3	−947.061968	−8.79	1.33	−13.81	5.02	−7.47
AB4	−947.061277	−8.35	10.77	−46.03	37.68	2.42
AB5	−947.061148	−8.28	2.16	−6.29	−1.99	−6.12
AB6	−947.060455	−7.84	0.71	−9.42	1.58	−7.14
AB7	−947.059224	−7.07	0.32	−9.99	2.92	−6.76
AB8	−947.059180	−7.04	2.13	−17.19	10.15	−4.92
Cysteine	−721.949023					
Urea	−225.273023					

[a] The total energy of complexes involve ZPVE and BSSE correction, while the energy of the monomers (cysteine and urea) involve ZPVE correction. All energies are in kcal mol^{-1} except the total energy (in Hartree).

4. Conclusion

The Cys–Urea complexes have been investigated at the ωB97XD/6-311++G(d,p) level. The nature of H-bonds was analyzed through structures, energies, frequencies and electron density topological analysis. Multiple H-bonds including intra- and intermolecular H-bonds are formed in complexes. The results show that the stability of Cys–Urea complexes is influenced by hydrogen bonding interactions and structural deformations. Although the strongest H-bond is involved, **AB4** is not the most stable complex due to the serious deformation. Similarly, **AB7** with the smallest ΔE_{prep} is also not the most stable complex, while **AB1** is the most stable complex since it involves the stronger hydrogen bonding interactions as well as the smaller deformation. The formations of most of complexes are helpful to strengthen the intramolecular O1H1A$\cdots$NA H-bond, which is attribute to the cooperativity of H-bond in complexes and can be learned from the results of structures, NBO and QTAIM. The electron density (ρ_b) and its Laplace ($\nabla\rho_b$) at BCPs significantly correlates with the H-bond parameter δRH$\cdots$Y. Moreover, a linearly relationship between the second-perturbation energies $E(2)$ and ρ_b have been found. In conclusion, we have presented evidence that the Cys–Urea complexes possess different types of intra- and intermolecular H-bonds. The variety of the hydrogen bonding motifs that occur in the studied complexes may be considerable important for the future molecular mechanism of urea-induced protein denaturation.

Acknowledgement

This work is supported by Tianjin Science and Technology Development Fund Projects in Colleges and Universities (No. 20080504).

References

[1] A. Wallqvist, D.G. Covell, D. Thirumalai, J. Am. Chem. Soc. 120 (1998) 427.
[2] M. Auton, L.M.F. Holthauzen, D.W. Bolen, Proc. Natl. Acad. Sci. USA 104 (2007) 15317.
[3] E.P. O'Brien, R.I. Dima, B. Brooks, D. Thirumalai, J. Am. Chem. Soc. 129 (2007) 7346.
[4] M.C. Stumpe, H. Grubmuller, J. Am. Chem. Soc. 129 (2007) 16126.
[5] A. Caballero-Herrera, K. Nordstrand, K.D. Berndt, L. Nilsson, Biophys. J. 89 (2005) 842.
[6] C. Oostenbrink, W.F. van Gunsteren, Phys. Chem. Chem. Phys. 7 (2005) 53.
[7] S.N. Timasheff, G.F. Xie, Biophys. Chem. 105 (2003) 421.
[8] M.E. Lee, N.F.A. van der Vegt, J. Am. Chem. Soc. 128 (2006) 4948.
[9] Y.P. Sun, X.H. Ren, H.J. Wang, Y.Y. Shan, L.J. Xing, Struct. Chem. 20 (2009) 213.
[10] A.K. Rappe, E.R. Bernstein, J. Phys. Chem. A 104 (2000) 6117.
[11] S. Grimme, J. Comput. Chem. 25 (2004) 1463.
[12] T. Schwabe, S. Grimme, Phys. Chem. Chem. Phys. 9 (2007) 3397.
[13] Y. Zhao, D.G. Truhlar, J. Phys. Chem. A 110 (2006) 5121.
[14] Y. Zhao, D.G. Truhlar, Theor. Chem. Acc. 120 (2008) 215.
[15] J.D. Chai, M. Head-Gordon, Phys. Chem. Chem. Phys. 10 (2008) 6615.
[16] E.R. Johnson, I.D. Mackie, G.A. DiLabio, J. Phys. Org. Chem. 22 (2009) 1127.
[17] L. Rao, H.W. Ke, G. Fu, X. Xu, Y.J. Yan, J. Chem. Theory Comput. 5 (2009) 86.
[18] K.E. Riley, M. Pitonak, J. Cerny, P. Hobza, J. Chem. Theory Comput. 6 (2010) 66.
[19] A.E. Reed, L.A. Curtiss, F. Weinhold, Chem. Rev. 88 (1988) 899.

[20] A.E. Reed, F. Weinhold, L.A. Curtiss, D.J. Pochatko, J. Chem. Phys. 84 (1986) 5687.
[21] R.F.W. Bader, Atoms in Molecules: A Quantum Theory, Oxford University Press, Oxford, U.K., 1990.
[22] P.L.A. Popelier, Atoms in Molecules: An Introduction, Pearson Education Limited, Edinburgh Gate, Harlow, England, 2000.
[23] C.F. Matta, R.J. Boyd, The Quantum Theory of Atoms in Molecules: From Solid State to DNA and Drug Design, Wiley-VCH Verlag GmbH & Co. KGaA, Weinheim, 2007.
[24] I. Alkorta, I. Rozas, J. Elguero, Chem. Soc. Rev. 27 (1998) 163.
[25] O. Mo, M. Yanez, J.E. Del Bene, L. Alkorta, J. Elguero, ChemPhysChem 6 (2005) 1411.
[26] I. Alkorta, J. Elguero, M. Solimannejad, J. Chem. Phys. 129 (2008).
[27] E. Espinosa, I. Alkorta, J. Elguero, E. Molins, J. Chem. Phys. 117 (2002) 5529.
[28] I. Alkorta, F. Blanco, J. Elguero, C. Estarellas, A. Frontera, D. Quinonero, P.M. Deya, J. Chem. Theor. Compt. 5 (2009) 1186.
[29] I. Alkorta, L. Barrios, I. Rozas, J. Elguero, J. Mol. Struct – (THEOCHEM) 496 (2000) 131.
[30] I. Alkorta, F. Blanco, J. Elguero, J. Phys. Chem. A 112 (2008) 6753.
[31] P.F. Provasi, G.A. Aucar, M. Sanchez, I. Alkorta, J. Elguero, S.P.A. Sauer, J. Phys. Chem. A 109 (2005) 6555.
[32] I. Alkorta, I. Rozas, J. Elguero, Struct. Chem. 9 (1998) 243.
[33] I. Rozas, I. Alkorta, J. Elguero, Struct. Chem. 19 (2008) 923.
[34] A.D. McLean, G.S. Chandler, J. Chem. Phys. 72 (1980) 5639.
[35] R. Krishnan, J.S. Binkley, R. Seeger, J.A. Pople, J. Chem. Phys. 72 (1980) 650.
[36] S.F. Boys, F. Bernardi, Mol. Phys. 19 (1970) 553.
[37] M.J. Frisch, G.W. Truchs, H.B. Schlegel, G.E. Scuseria, M.A. Robb, J.R. Cheeseman, V.G. Zakrzewski, J.A. Montgomery Jr., R.E. Stratmann, J.C. Burant, S. Dapprich, J.M. Millam, A.D. Daniels, K.N. Kudin, M.C. Strain, O. Farkas, J. Tomasi, V. Barone, M. Cossi, R. Cammi, B. Mennucci, C. Pomelli, C. Adamo, S. Clifford, J. Ochterski, G.A. Petersson, P.Y. Ayala, Q. Cui, K. Morokuma, D.K. Malick, A.D. Rabuck, K. Raghavachari, J.B. Foresman, J. Cioslowski, J.V. Ortiz, A.G. Baboul, B.B. Stefanov, G. Liu, A. Liashenko, P. Piskorz, I. Komaromi, R. Gomperts, R.L. Martin, D.J. Fox, T. Keith, M.A. Al-Laham, C.Y. Peng, A. Nanayakkara, C. Gonzalez, M. Challacombe, P.M.W. Gill, B. Johnson, W. Chen, M.W. Wong, J.L. Andres, C. Gonzalez, M. Head-Gordon, E.S. Replogle, J.A. Pople, Gaussian03, Gaussian, Inc., Pittsburgh, PA, 2003.
[38] F. Biegler-König, AIM2000, University of Applied Sciences, Bielefeld, Germany, 2000.
[39] J.J. Wilke, M.C. Lind, H.F. Schaefer, A.G. Csaszar, W.D. Allen, J. Chem. Theory Comput. 5 (2009) 1511.
[40] J.C. Dobrowolski, J.E. Rode, J. Sadlej, J. Mol. Struct. (THEOCHEM) 810 (2007) 129.
[41] J.C. Dobrowolski, M.H. Jamroz, R. Kolos, J.E. Rode, J. Sadlej, ChemPhysChem 8 (2007) 1085.
[42] M. Pecul, Chem. Phys. Lett. 418 (2006) 1.
[43] P.L.A. Popelier, J. Phys. Chem. A 102 (1998) 1873.
[44] S.X. Tian, J. Phys. Chem. B 108 (2004) 20388.
[45] A. Bondi, J. Phys. Chem. 68 (1964) 441.
[46] Y. Hannachi, B. Silvi, Y. Bouteiller, J. Chem. Phys. 97 (1992) 1911.
[47] O. Mo, M. Yanez, J. Elguero, J. Chem. Phys. 97 (1992) 6628.
[48] H.S. Frank, W.Y. Wen, Discuss. Faraday Soc. 24 (1957) 133.
[49] O. Galvez, P.C. Gomez, L.F. Pacios, J. Chem. Phys. 118 (2003) 4878.
[50] R. Miao, C. Jin, G.S. Yang, J. Hong, C.M. Zhao, L.G. Zhu, J. Phys. Chem. A 109 (2005) 2340.
[51] A.G. Nozad, S. Meftah, M.H. Ghasemi, R.A. Kiyani, M. Aghazadeh, Biophys. Chem. 141 (2009) 49.
[52] R.L.T. Parreira, H. Valdes, S.E. Galembeck, Chem. Phys. 331 (2006) 96.
[53] H.W. Zhou, W.P. Lai, Z.Q. Zhang, W.K. Li, H.Y. Cheung, J. Comput. – Aided Mol. Des. 23 (2009) 153.
[54] U. Koch, P.L.A. Popelier, J. Phys. Chem. 99 (1995) 9747.
[55] W.D. Arnold, E. Oldfield, J. Am. Chem. Soc. 122 (2000) 12835.
[56] L.F. Pacios, J. Phys. Chem. A 108 (2004) 1177.